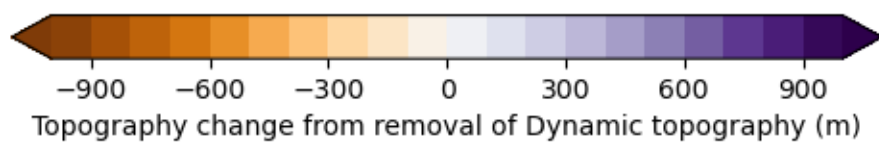
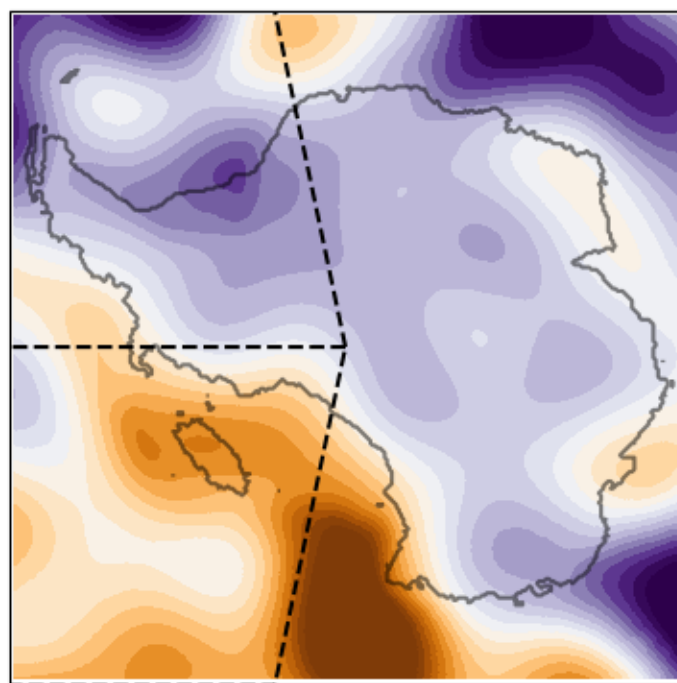
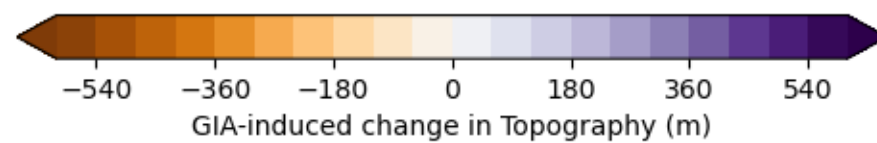
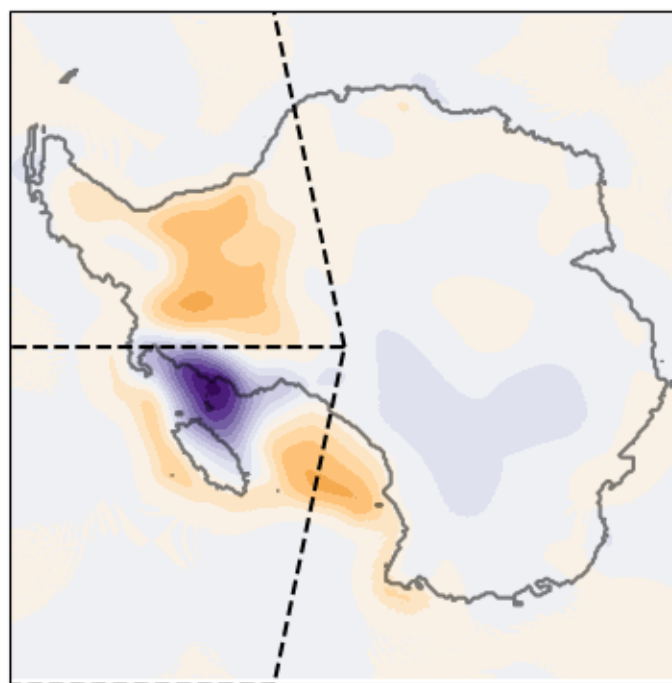


Figure 1.

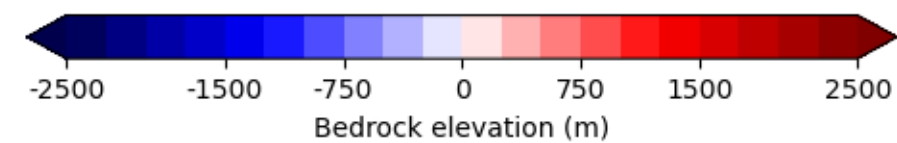
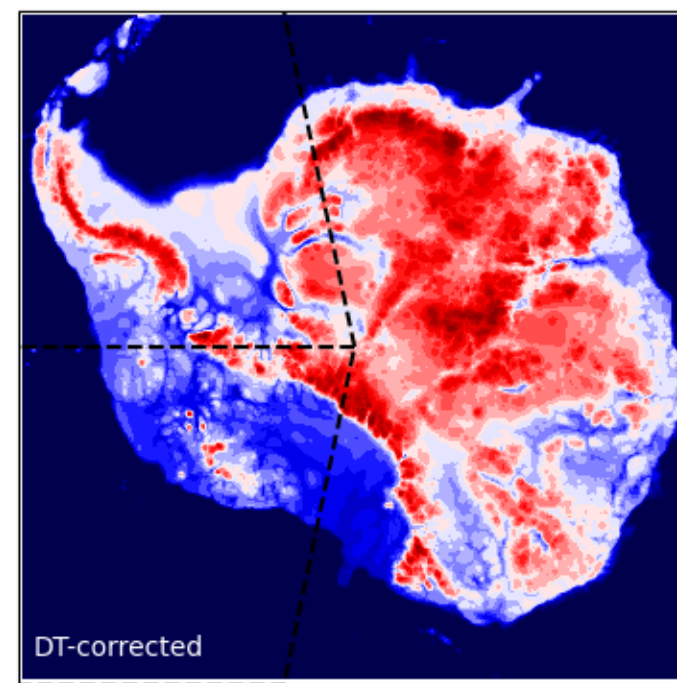
A)



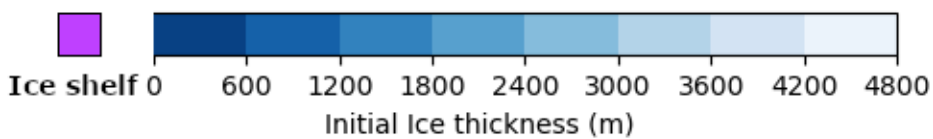
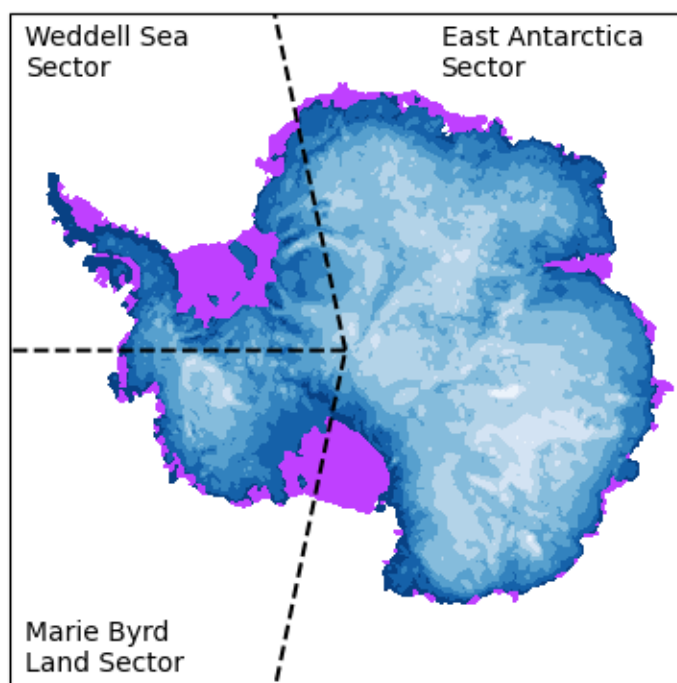
B)



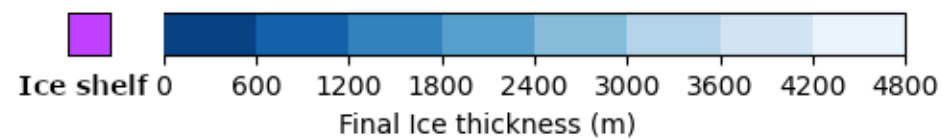
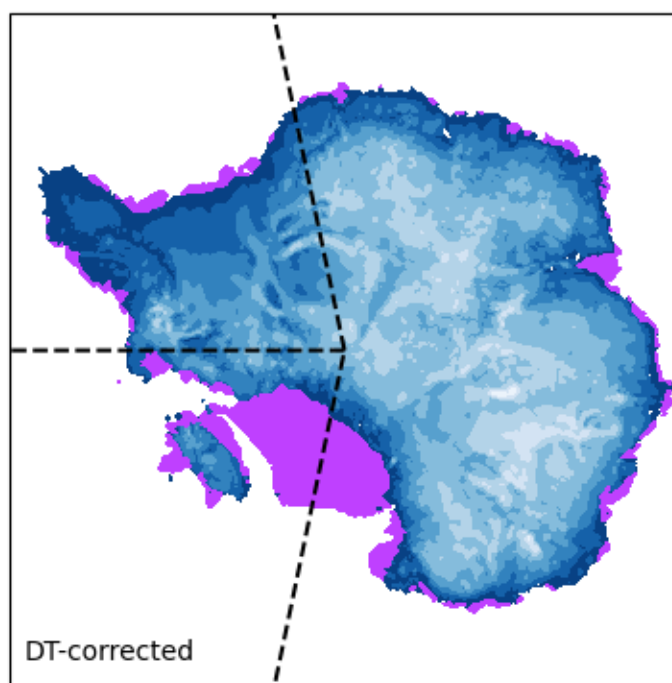
C)



D)



E)



F)

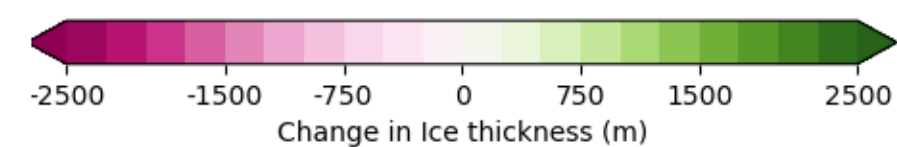
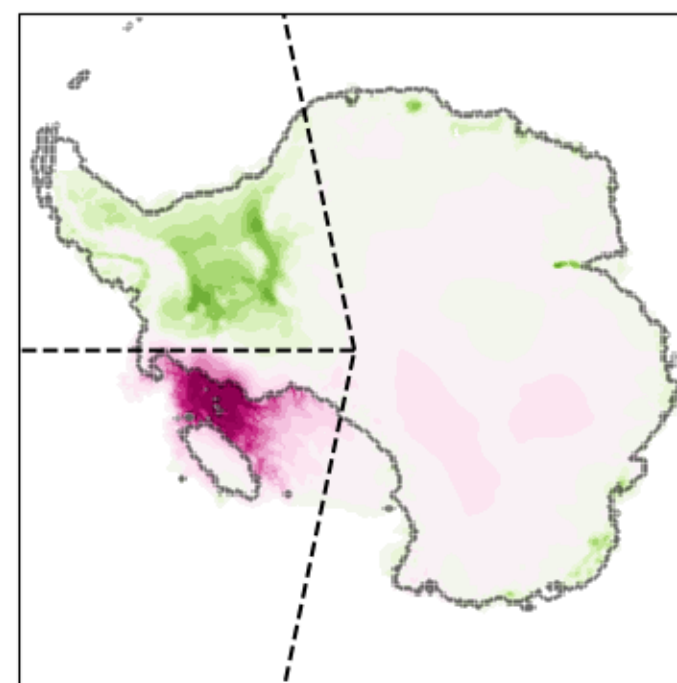
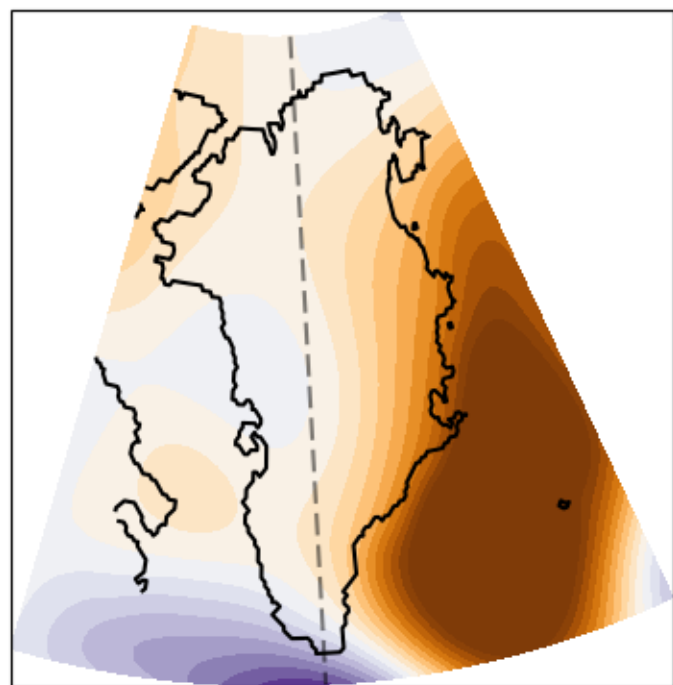


Figure 2.

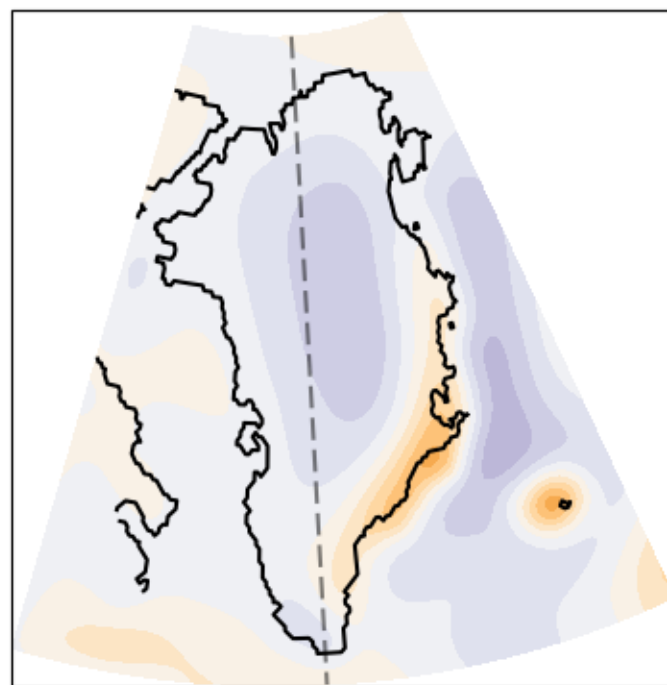
A)



-900 -600 -300 0 300 600 900

Topography Change from Removal of Dynamic Topography (m)

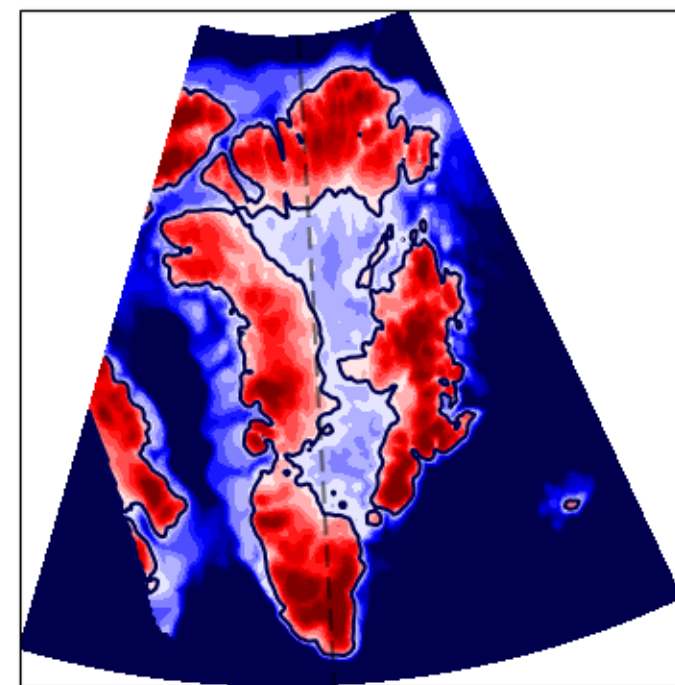
B)



-225 -150 -75 0 75 150 225

GIA-induced change in Topography (m)

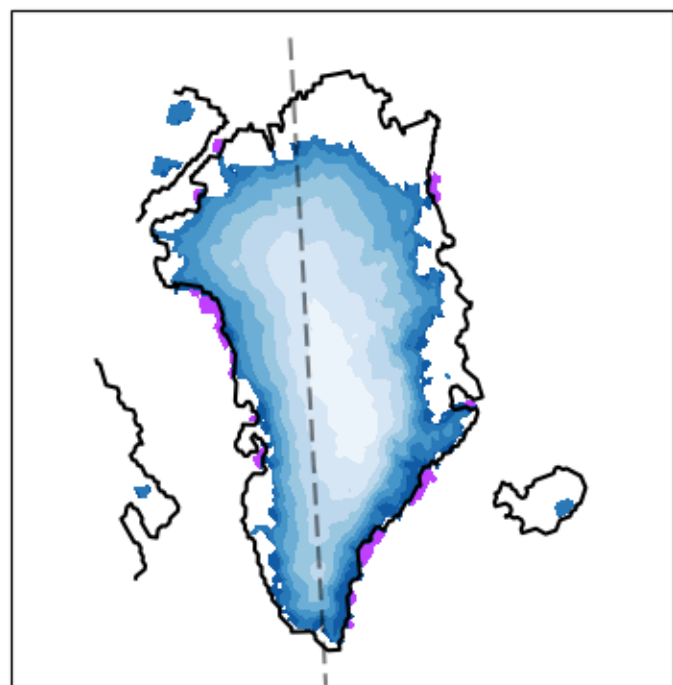
C)



-1000 -600 -300 0 300 600 1000

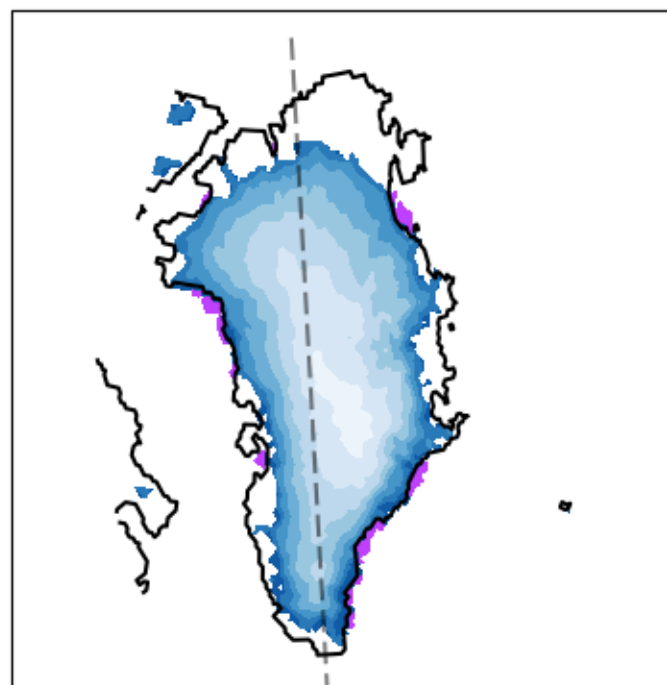
Bedrock elevation (m)

D)



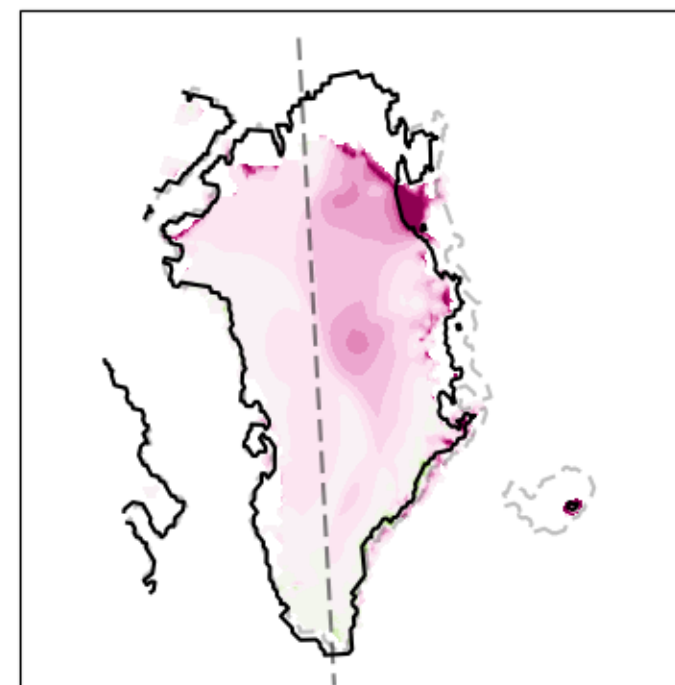
Ice Shelf
0 400 800 1200 1600 2000 2400 2800 3200
Initial Ice thickness (m)

E)



Ice Shelf
0 400 800 1200 1600 2000 2400 2800 3200
Final Ice thickness (m)

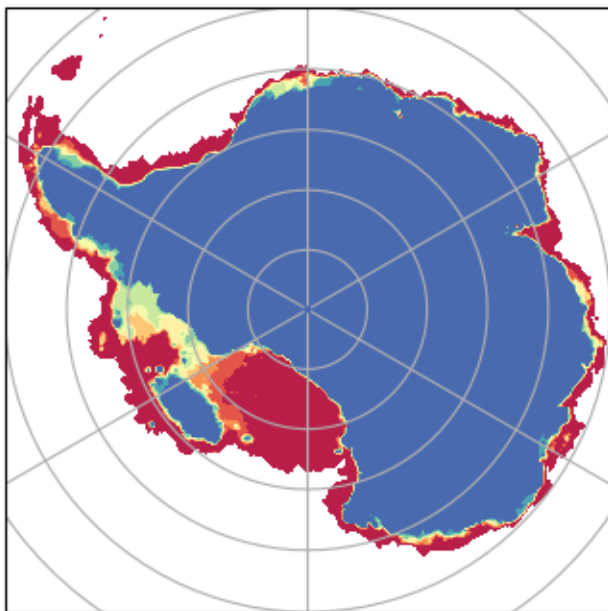
F)



-600.0 -360.0 -180.0 0.0 180.0 360.0 600.0
Change in Ice thickness (m)

Figure 3.

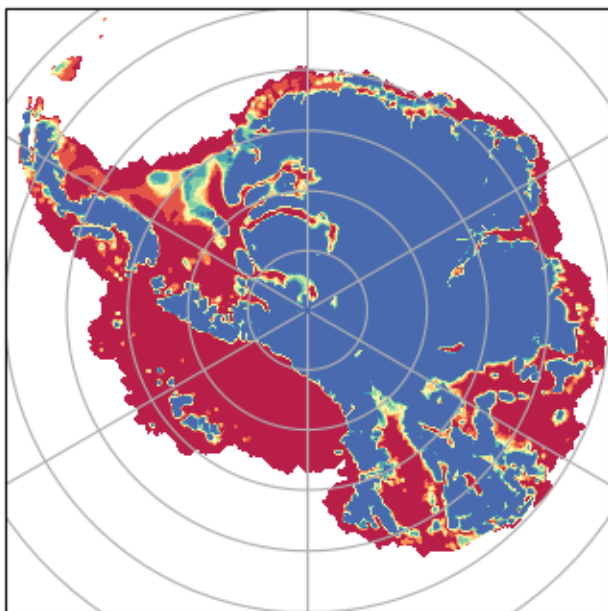
A) Probability of grounded ice at end of simulation



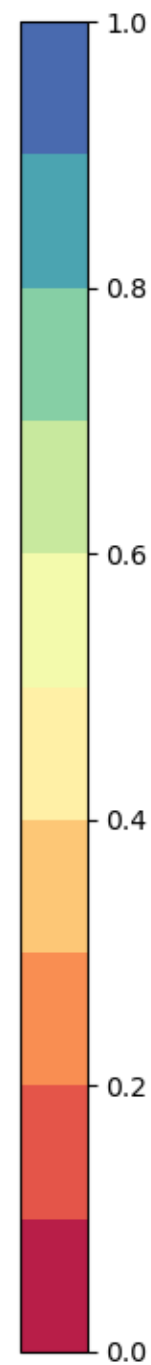
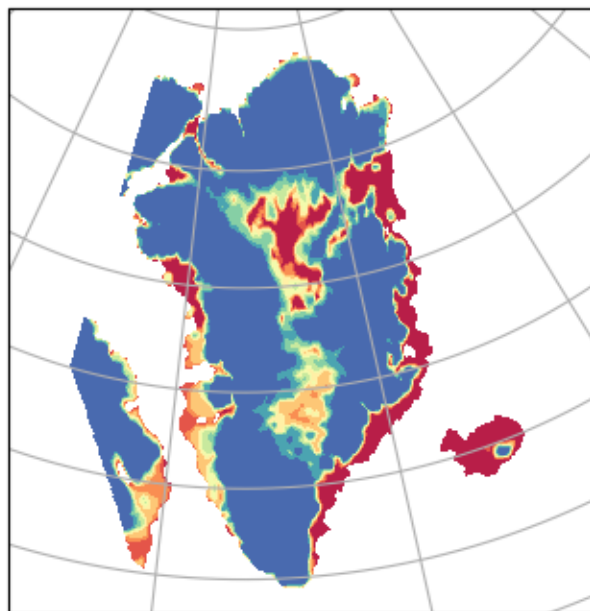
B) Probability of grounded ice at end of simulation



C) Probability of bedrock above sea level at end of simulation



D) Probability of bedrock above sea level at end of simulation



Ice Sheets Without Dynamic Topography

B. Parazin¹, Natalya Gomez¹, Fred Richards², Mark J. Hoggard³, Sophie Coulson⁴,
Jerry Mitrovica⁵

¹McGill University, Department of Earth and Planetary Sciences

²Imperial College London, Department of Earth Science and Engineering

³Australian National University, Research School of Earth Sciences

⁴University of New Hampshire, Department of Earth Sciences

⁵Harvard University, Department of Earth and Planetary Sciences

Key Points:

- We perform simulations of the Greenland and Antarctic Ice Sheets where present-day dynamic topography is removed and ice sheets reach new equilibria
- We demonstrate that present-day dynamic topography plays a crucial role in determining the equilibrium geometries of modern ice sheets
- Our results have implications for earlier icehouse climates, where dynamic topography would be important but is much more uncertain

Corresponding author: B. Parazin, bc.parazin@mail.mcgill.ca

Abstract

Dynamic topography results in uplift and subsidence events on Earth’s surface with amplitudes on the order of a kilometer. These vertical motions are known to have influenced ice sheet evolution, but how dynamic topography has controlled the current state of present ice sheets is unknown. Here, we explore this by running ice sheet models to their equilibrium state after removing present-day dynamic topography. We find that Antarctic ice cover is significantly different without dynamic topography; in our optimal dynamic topography model, the ice mass (grounded area) in Marie Byrd Land decreases by 58% (55%), while the ice mass (grounded area) in the Weddell Sea increases 55% (77%). In Greenland, we see ice loss in the east and, in our optimal dynamic topography model, large sectors of the ice sheet become marine-based. Taken together, these findings indicate that dynamic topography plays a major role in the equilibrium geometries of ice sheets.

Plain Language Summary

Mantle flow can exert a vertical force on overlying crust, and this force can raise or lower the crust by ~ 1 km over a few million years. Ice sheet steady-state positions are highly influenced by the elevation of the bedrock they sit on, and any process that raises or lowers the crust beneath ice sheets can drive long-term changes in ice cover. Previous research has shown that the impact of mantle flow on bedrock elevation played a role in establishing the geometry of the Greenland Ice Sheet ~ 3 million years ago, but the extent to which crustal elevation supported by mantle flow impacts the steady-state geometry of modern ice sheets is unknown. To answer this question, we simulated the steady-state positions of the Antarctic and Greenland Ice Sheets after removing this mantle support. Using an optimally performing model, we find that West Antarctic ice cover is dramatically changed, with a $\sim 50\%$ redistribution of ice mass. In Greenland, there is significant ice loss on the east coast, and large sections of the interior are exposed to the ocean, becoming marine-based ice. These results demonstrate that the mantle support of bedrock elevation under ice sheets is fundamentally important in determining their steady-states.

Keywords

Dynamic topography, Ice sheets, Glacial isostatic adjustment

1 Introduction

Bedrock topography underlying an ice sheet is important in determining the evolution and equilibrium states of the overlying ice (e.g. Ignéczi et al., 2018; Morland & Johnson, 1982; Paxman et al., 2020). Changes in the elevation of the bed impact the elevation of the surface of the ice and thus its surface climate (e.g. Weertman, 1961; Zeitz et al., 2022), the flow pattern of grounded ice over the bed (e.g. Cooper et al., 2019; Morlighem et al., 2017, 2020) and the flux of ice across the grounding line in marine-based sectors (e.g. Mercer, 1978; Schoof, 2007; Weertman, 1974). On a retrograde slope (a bed that deepens towards the interior of the ice sheet), there is generally no stable grounding line position for a retreating ice sheet, leading to a phenomenon known as marine ice sheet instability (MISI) whereby marine-grounded ice sheets on retrograde slopes will retreat until they reach a local topographic high known as a pinning point (Durand et al., 2009; Robel et al., 2019; Schoof, 2007; Weertman, 1974).

Many solid Earth processes act to shape bedrock topography and impact ice sheets on different spatiotemporal scales, including glacial isostatic adjustment (GIA) (e.g. Coulon et al., 2021; Gomez et al., 2010, 2024), subglacial erosion and deposition (e.g. Colleoni et al., 2018; Paxman et al., 2019, 2020), and, on timescales longer than ~ 100 kyr, dynamic topography (Austermann et al., 2015). Dynamic topography is the deviation of the solid Earth’s surface elevation from isostatic equilibrium driven by mantle convective flow (Braun, 2010). While the earliest studies of dynamic topography focused on issues related to long-term sea level change and sedimentary basin development (e.g. Gurnis, 1990; Hager et al., 1985; Mitrovica et al., 1989), recent studies have described myriad connections between dynamic topography and ice age paleoclimate, with broad implications for ocean chemistry and circulation, biodiversity, ecology and the cryosphere (see Mitrovica et al. (2020), for a comprehensive review).

Austermann et al. (2015) modeled dynamic topography and reconstructed Antarctic bedrock topography changes since the mid-Pliocene warm period, 3 million years ago. They combined an equilibrium ice sheet model with the reconstructed topography and mid-Pliocene climate forcing and predicted significant retreat of the ice margin in the Wilkes sub-glacial basin, in accord with a range of geological evidence. Steinberger et al. (2015) modeled dynamic topography change in the North Atlantic over the last 5 million years and found that uplift from the Iceland plume and true polar wander pre-conditioned glacial inception in Greenland. Coulson (2021) modeled dynamic topography variations across the Canadian archipelago covering the same time period, and reconstructed significant, ≈ 100 m, uplift over Northeast Baffin Island, also preconditioning inception of the North American glaciation. Finally, Fox et al. (2024) estimated over a kilome-

ter of uplift of the northern Antarctic Peninsula using an inverse analysis of pre-glaciation fluvial networks, and argued that this drove onset of glaciation in the region ≈ 10 million years ago.

These studies demonstrated the importance of dynamic topography as a driver of ice sheet evolution in the Neogene, but they also raised an intriguing question: How important is dynamic topography in modulating present-day ice cover over the Antarctic and Greenland? That is, what would present-day polar ice sheet extent be in the absence of topography supported by thermochemical convection in the Earth’s mantle? A comprehensive analysis of globally distributed seismic surveys of oceanic crust indicated that present-day residual topography – a proxy for dynamic topography – is characterized by amplitudes of ± 1 km and spatial scales of ≈ 1000 km (Hoggard et al., 2017), and this inference is supported by numerical modeling of the convection process constrained by a range of geological and geophysical observables (e.g. Davies et al., 2019; Richards et al., 2023, 2020; Steinberger, 2016). This signal is comparable in both magnitude and scale to dynamic topography changes that have been linked, in work cited above, to critical events in the past evolution of the cryosphere.

Herein we address the above question by modeling the impact of dynamic topography on the present-day equilibrium state of the Greenland and Antarctic Ice Sheets. We perform a suite of coupled ice sheet – GIA model simulations of each ice sheet with fixed modern climate. In these simulations, a predicted present dynamic topography signal (Richards et al., 2023) is removed and the ice sheets evolve to reach new equilibria. Our model captures both the direct impact of dynamic topography on ice sheet evolution through its effect on bedrock elevation, as well as its indirect impact via GIA processes (Austermann & Mitrovica, 2015). We further determine the sensitivity of the equilibrium reached to variations in predicted present-day topography, and demonstrate the relative importance of lower and upper mantle stresses in establishing the present-day equilibrium state. Our findings identify dynamic topography as a significant pathway through which mantle dynamics influence ice sheet stability, sea level and climate on Earth’s surface, with important implications for studies of previous icehouse periods.

2 Methods

We apply the coupled ice sheet – GIA model of Gomez et al. (2013, 2015) to perform our analysis with fixed modern climate, and utilize the predicted present-day dynamic topography signal from Richards et al. (2023, see their figure 2h). Furthermore, we augment the coupled model to incorporate a method for considering the solid Earth response to dynamic topography and associated ice sheet changes described in Austermann & Mitrovica (2015). In the following sections, we describe these models and the configuration of the coupled simulations.

2.1 Ice Sheet Modeling

We adopt the PSUICE3D model, described in Pollard & DeConto (2012a, 2020), to simulate ice sheet evolution. PSUICE3D uses a combination of the shallow ice and shallow shelf approximations to handle regimes where vertical shear stresses and longitudinal stresses dominate respectively, with the grounding line parameterized following Schoof (2007). Parameterizations are also included for sub-ice-shelf melt (Albrecht et al., 2011) and calving flux (Nick et al., 2010). PSUICE3D implements a Weertman-type basal sliding law, with different treatments of basal sliding coefficients below modern grounded and oceanic areas (see below). A degree-day scheme is used to calculate surface melt. Surface mass balance (SMB) is taken to be the difference between snowfall and surface melt and the model does not consider firn processes. All ice sheet simulations are performed with 1-year time stepping.

We use a 20-km square south polar stereographic grid to model Antarctica. The initial Antarctic bedrock topography and ice thicknesses are given by Bedmap2 (Fretwell et al., 2013). Preliminary tests with PSUICE3D (not shown here) suggest that adopting the newer Bedmachine model of bedrock topography (Morlighem et al., 2020) lead to negligible differences on the continental scale.

When modeling Greenland, a 0.2 degrees latitude by 0.4 degrees longitude grid is used. This is equivalent to ~ 22 km latitudinal spacing and longitudinal spacing which varies from ~ 22 km at the southern limit of the ice sheet (60.1°N) to ~ 6 km at the northern limit of the ice sheet (82.1°N). The initial topography and ice thicknesses follow that of Bamber et al. (2013).

The SMB is derived from pre-industrial, present-day atmospheric data from ALBMAP (Le Brocq et al., 2010) for Antarctica and the RACMO 2.3 climate model (Noël et al., 2018; van Meijgaard et al., 2008) for Greenland. Face melt rate is calculated using modern temperatures from the World Ocean Atlas 2009 (Levitus et al., 2012).

Basal sliding coefficients are determined through an iterative procedure detailed in Pollard & DeConto (2012b) under present-day grounded ice and set to $10^{-5} \text{ m a}^{-1} \text{ Pa}^{-2}$ in modern oceanic regions for simulations shown in the main text following Pollard et al. (2016, 2017), and to $10^{-6} \text{ m a}^{-1} \text{ Pa}^{-2}$ in some sensitivity tests shown in supplemental materials (see figures S12 and S13).

2.2 GIA Modeling

To simulate GIA we adopt the gravitationally self-consistent, pseudo-spectral sea level algorithm described in Kendall et al. (2005) and Gomez et al. (2010) with the implementation of a time window algorithm (Han et al., 2022) to improve processing times. The global model ac-

counts for shoreline migration and gravitational, rotational and deformational perturbations driven by ice-ocean mass transfer on an Earth with mechanical properties that vary with depth alone. We implement the extensions to the general sea level equation (Mitrovica & Milne, 2003) described by Austermann & Mitrovica (2015), which solves for the long-term (isostatic equilibrium) adjustment of sea level driven by dynamic topography and ice mass changes. In this analysis, we neglect the sea level impact of perturbations in Earth rotation directly associated with dynamic topography, as these would be small compared to changes associated with dynamic topography and GIA. Rotational effects from changes in ice distribution are still considered.

Initial topography is provided by ETOPO2 (NGDC, 2006) outside the ice sheet model domain and is set to the ice sheet model’s initial bedrock elevation within the domain. The ice history outside the model domain is held at the present value of the ICE_6GC model (Argus et al., 2014; Peltier et al., 2015), while in the domain it is provided by the ice sheet model.

We adopt an Antarctic lithosphere thickness of 50 km, consistent with observational evidence for West Antarctica (e.g. Barletta et al., 2018; Lloyd et al., 2020), and a lithosphere thickness in Greenland of 120 km taken from the inversions performed in Lecavalier et al. (2014). We consider other values in supplementary sensitivity tests (see figures S12 and S13). On the timescale of dynamic topography, isostasy can be modeled as an elastic surface over an inviscid substrate, and thus we treat the mantle as inviscid in all simulations. This contrasts with most GIA simulations, which model a non-zero mantle viscosity.

2.3 Dynamic Topography Model

The predicted dynamic topography field (figure S1) in our optimal calculation is taken from Richards et al. (2023) and was generated using the spectral method pioneered by Hager & O’Connell (1981) and extended by Corrieu et al. (1995). The density model underpinning this calculation has been optimized to fit a suite of geodynamic, geodetic, and seismic observations, and details of how it was produced can be found in supplemental methods section S1 or Richards et al. (2023). Our optimal model is derived from Richards et al. (2023)’s compositional inversions that adopt the TX2011 shear velocity structure (Grand, 2002) to infer densities and the S10 radial viscosity profile of Steinberger et al. (2010). When quantifying the sensitivity to variations in dynamic topography, we repeat the analysis described below with the remaining 14 geodynamic inversion models described in Richards et al. (2023, section S1). In supplemental tests, dynamic topography fields only corresponding to the upper and lower mantle are generated (see figures S10 and S11). This procedure is also described in detail in supplementary material.

2.4 Coupling method and simulation setup

To achieve an initial modern equilibrium state, a 15,000 year spin up simulation is performed prior to the removal of dynamic topography with constant pre-industrial present climate forcing using the coupled ice sheet-GIA model and the modern bedrock topography described above. The spun-up states are shown in figures 1D and 2D, demonstrating the model reasonably reproduces current ice sheet conditions. Starting from this modern equilibrated state, 30,000-year simulations with constant modern climate are performed in which the dynamic topography signal is removed linearly over the first 10,000 years for Greenland or the first 20,000 years for Antarctica (for increased numerical stability), and the model subsequently reaches a new equilibrium state. The procedure for removing the whole-mantle, upper-mantle and lower-mantle dynamic topography signals is the same. Supplemental figures S14-S16 demonstrate that there is little difference in the final equilibrium state if dynamic topography is instead removed before performing a spin up. This is important, since it implies any future studies can add dynamic topography to already-spun-up ice sheet models without introducing significant error.

Because the GIA model covers a global domain, worldwide dynamic topography is removed, and the corresponding changes in global mean sea level that result from its removal altering ocean volume and seafloor position are automatically considered in addition to the local topographic changes. Mean ocean-loaded dynamic topography (MOLDT) over the oceans for all dynamic topography models used is listed in table S3. For all 15 models, MOLDT is positive, so dynamic topography is supporting a higher global mean sea level; that is, removing dynamic topography would cause a global mean sea level drop approximately equal to the MOLDT value the table. Several processes that may be impacted by dynamic topography are not considered in our modeling, including changes in chemical weathering rates, erosion and sedimentation, and atmospheric circulation.

The GIA model is called by the ice sheet model to update bedrock topography every 100 model years, applying both the dynamic topography change and any changes due to GIA. To reduce computational cost, an evolving time window is applied. At the time of the GIA model call, the previous 10,000 years are sampled with a period of 100 years (i.e. the coupling time), and, moving progressively backwards, there are further sections of 5000, 5000, and 10000 years sampled with periods of 200, 500 and 1000 years respectively. See Han et al. (2022) for an in-depth description of this method. Calculations are performed up to spherical harmonic degree and order 512.

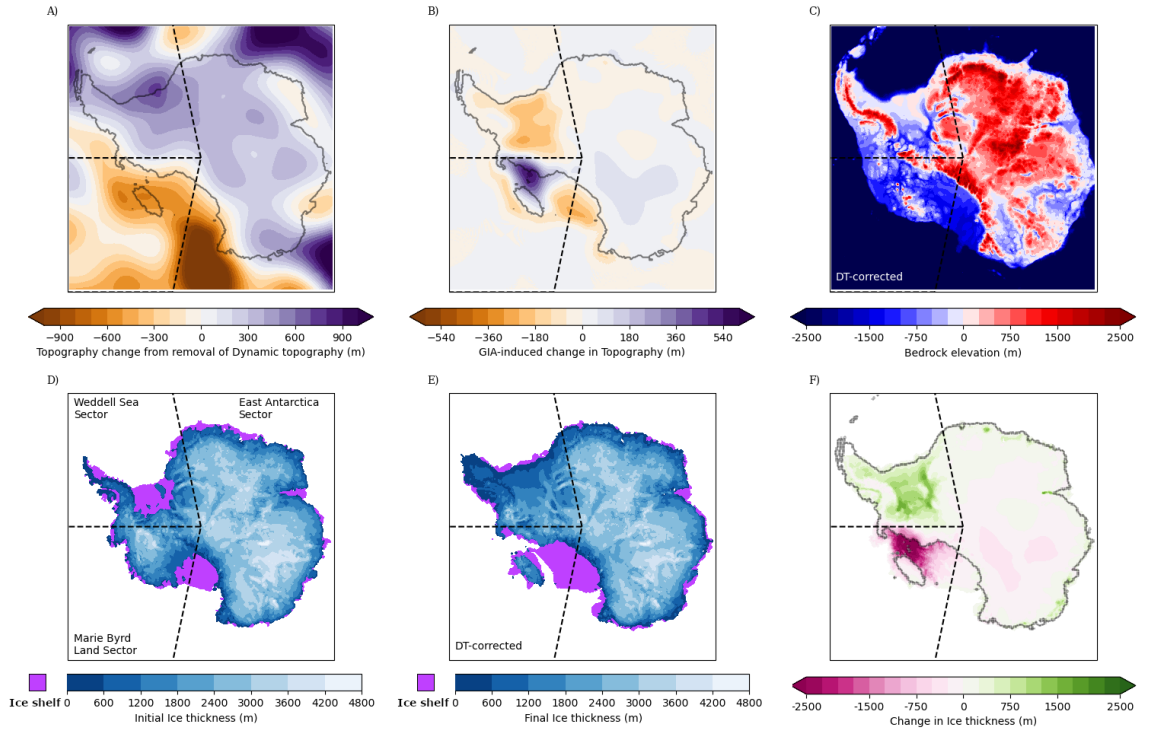


Figure 1. Effect of removing the present-day predicted signal of the optimal dynamic topography model from Antarctica. (A) Predicted change in bedrock topography beneath the modeled Antarctic ice sheet due to dynamic topography effects. This includes amplification from water loading and changes in sea level due to ocean volume and sea floor position changes. (B) Change in bedrock topography beneath the modeled ice sheet from GIA (i.e. total bedrock change-1A). The grounding line of the final ice sheet state is outlined in black. (C) The final state of bedrock topography after the dynamic topography signal is removed in an isostatically self-consistent manner. (D) The initial ice thickness following the pre-industrial modern spin up, and (E) final ice thickness after isostatically self-consistent dynamic topography removal. Areas of ice shelf are colored in purple. (F) The difference in grounded ice thickness between the final and initial equilibrium states (i.e. E minus D). The grounding line of the final dynamic topography-free ice sheet is shown in grey.

3 Results

3.1 Antarctica

The removal of the present day dynamic topography signal and associated GIA effects from bedrock elevation beneath Antarctica leads to net subsidence in the Marie Byrd Land sector and uplift in the Weddell sea sector (figures 1A-B). The average topography change over the continental shelf of the Marie Bryd Land sector (as labeled in figure 1D) is ~ -330 m (figure 1A), but some regions near the border with the Weddell Sea sector experience GIA uplift in response to large-scale local ice sheet retreat (figures 1B, 1F). Broad uplift occurs over much of the Weddell Sea sector, with an average increase in elevation of ~ 260 meters across the continental shelf. East Antarctica overall experiences topographic uplift due to dynamic topography and GIA (figure 1A-B) driven by moderate ice loss in the continental interior (figure 1F).

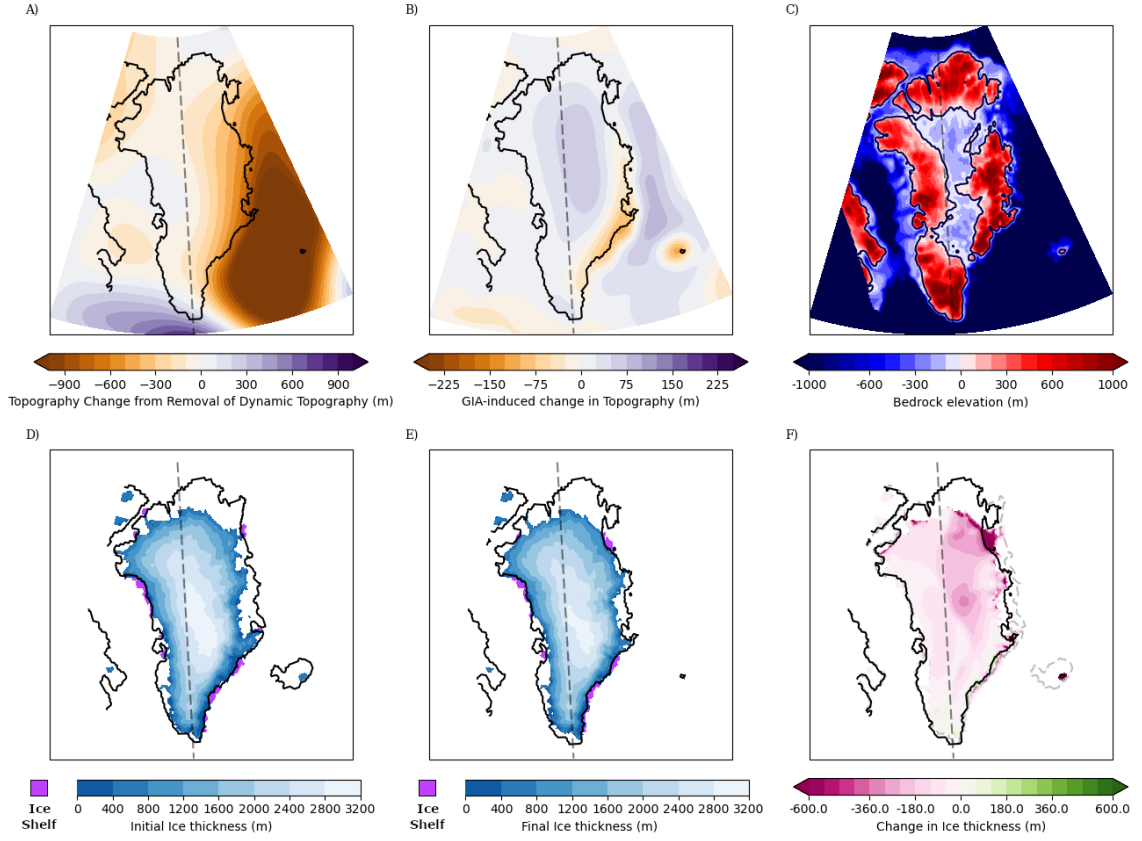


Figure 2. As in figure 1, except for the Greenland Ice Sheet. The dashed line in frames A-F (45° east longitude) separates east and west Greenland for the purposes of discussion and instead of showing the grounding line, the black outline shows the coastline. Additionally, the original coastline is shown as a dashed line in frame F. Though comparing figures D and E shows the ice is closer to coastline after dynamic topography is removed (frame E), this is because removing dynamic topography has caused the coastline to retreat to the west, not because there was ice growth.

The removal of the dynamic topography signal leads to a significant redistribution of ice, especially in West Antarctica (see figures 1D, 1E, and 1F). Bedrock uplift in the Weddell Sea sector causes ice to grow out to the edge of the continental shelf, with an increase in ice mass (grounded ice area) of 55% (77%) within this sector. The Marie Byrd land sector sees a loss of 58% (55%) of its initial ice mass (grounded ice area) due to MISI, as removing the dynamic topography signal increases sea level at marine grounding lines. East Antarctica sees a net decrease in ice mass of 2.2%, but an increase in grounded ice area of 4.2% (figure 1F), likely due to a decrease in precipitation in the interior and an increase in precipitation falling on the coasts as the ice sheet is uplifted.

3.2 Greenland

In Greenland, the dynamic topography signal is dominated by a large high associated with the Iceland hot spot track. Removing it causes significant subsidence along the east coast of the

island (see figure 2A), which peaks at ≈ 1400 m in the southeast. This subsidence opens channels in the northwest, northeast and southeast of Greenland (figure 2C) which connect low topography in the interior of the island to the ocean, causing large sections of the interior Greenland ice sheet to become marine-based ice, i.e. ice grounded on bedrock that both lies below sea level and has a connection to the ocean.

When removing the dynamic topography signal, the general trend in Greenland is ice loss, except for a small amount of ice gain in the southern extremes (figure 2F). The ice sheet sees an ice mass decrease of 7.9%, and a grounded ice area decrease of 8.0% with the majority of the ice loss ($\sim 75\%$) occurring along the east coast where topographic subsidence is largest (figure 2F). The subsidence causes the coastline in the northeast, around the terminus of the Northeast Greenland Ice Stream, to retreat inland further than the easternmost extent of the ice. Any ice seaward of a pinning point melts due to MISI, accounting for $\sim 33\%$ of the total ice loss over Greenland. Over the remainder of the ice sheet, modest ice loss occurs due to ice-elevation feedback, driven by relative subsidence across the island resulting from removal of the present-day positive dynamic topography signal (figure 2A). This effect is moderated by GIA, which contributes topographic uplift in response to ice loss (figure 2B).

3.3 Sensitivity tests

3.3.1 Sensitivity to Choice of Dynamic Topography Model

To quantify the sensitivity of ice sheets to uncertainty in present-day dynamic topography models, we repeat the above analysis for 14 other present-day dynamic topography models considered in Richards et al. (2023) and use them in addition to the above results to produce a series of misfit-weighted probabilities of the equilibrium ice sheet state (see figure 3; figure S3 shows the weights applied to each model). In addition to the analysis shown below, supplemental figures S4, S5 and S6 show the results of all 15 Antarctica simulations, and S7, S8 and S9 provide the results of all 15 Greenland simulations.

The most dramatic changes observed in Antarctica following the removal of the best-fit dynamic topography signal are robust. Without the effects of dynamic topography, the Antarctic Ice Sheet extends consistently up to the Weddell Sea shelf, and retreats from its present-day position in Marie Byrd Land, though there is variability in the extent of retreat. The misfit-weighted probability of both results is nearly 1.0. The probability of a grounded-ice free corridor forming between the Amundsen and Ross Seas is somewhat less, ~ 0.58 (see figure 3A).

There is less variability in the final Greenland Ice Sheet configuration across the simulations, with the exception of the area around the terminus of the Northeast Greenland Ice Stream.

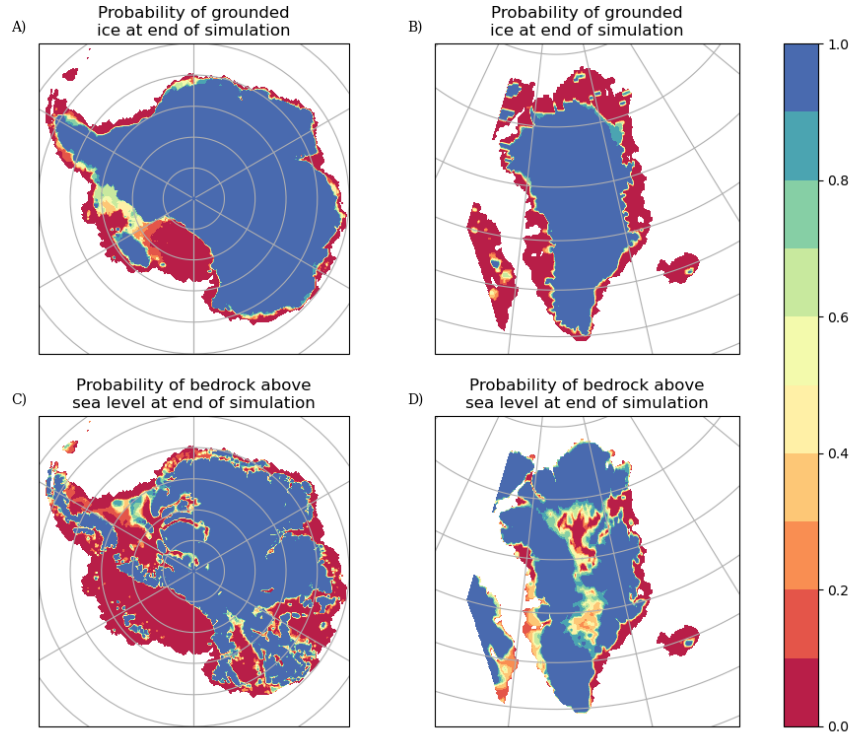


Figure 3. Sensitivity to choice of dynamic topography model. Frame A and B show the dynamic topography model misfit-weighted probability of each grid cell containing grounded ice upon reaching a new equilibrium state. Frames C and D shows the dynamic topography model misfit-weighted probability of the topography in each grid cell being above sea level after achieving equilibrium. In all frames, the area which is ice-shelf-free ocean for the duration of the simulation is masked out. Supplemental figure S3 shows the weights applied to each dynamic topography model.

In that area, there is a ~ 0.21 chance of the retreat observed when using the optimal dynamic topography model (figure 3B). The probability of sufficient subsidence occurring to open a channel from the ocean to the interior low-topography areas and convert the interior of Greenland into marine-based ice, as predicted using the best-fit model of dynamic topography, is only ~ 0.25 (figure 3D). The low probabilities arise because the optimal dynamic topography model has one of the highest magnitude signals over East Greenland and a near-zero dynamic topography signal over West Greenland, where most other models have a moderate to large negative signal (see figure S9).

3.3.2 Sensitivity to Stresses in the Lower and Upper Mantle

In supplementary material, we show the results of simulations in which we isolate upper and lower mantle contributions to dynamic topography and demonstrate that both influence the

overlying ice cover significantly (figures S2, S10 and table S1). We briefly discuss the results here. In the case of Antarctica, the total change in ice sheet mass in the upper-mantle-only simulation is -1.6×10^6 gigatonnes, while the lower-mantle-only simulation yields a change of 2.0×10^6 gigatonnes. The sum of the changes in mass from the upper and lower mantle is $\sim 4.0 \times 10^5$ gigatonnes, $\sim 10^6$ gigatonnes greater than the overall change of -7.4×10^5 gigatonnes in the whole-mantle simulation, pointing to significant non-linear coupling between bedrock elevation and ice sheet stability. Similar results are obtained when adopting a different location for the upper/lower mantle boundary (figure S11A-D, table S2). In the case of Greenland, both partial-mantle simulations have approximately half the ice loss of the whole mantle simulation, but there are still important local non-linear effects around the terminus of the Northeast Greenland Ice Stream where the ice loss in the whole-mantle simulation is greater than the combined losses from simulations with dynamic topography determined from models based on upper and lower mantle heterogeneity alone. Greenland shows a similar insensitivity to the adopted location of the division between upper and lower mantle (figure S11E-H).

4 Discussion and conclusion

We find that dynamic topography plays a key role in modulating the present-day equilibrium state of Earth’s ice sheets. In Antarctica, with dynamic topography removed, there is major redistribution of ice. There is a high probability of significant retreat and a ~ 0.58 chance of an almost complete loss of marine-based ice from Marie Byrd Land due to MISI. The advance of ice to the continental shelf in the Weddell Sea sector is seen in almost all models. In Greenland, subsidence associated with the removal of the dynamic topography signal leads to an 8% decrease in ice volume due to ice-elevation and MISI feedbacks in our optimal dynamic topography model, and converts much of interior Greenland into a marine-based ice sheet. However, the latter is not common in the additional dynamic topography models considered here. Finally, we find that the present-day ice sheets are non-negligibly dependent on dynamic topography driven by both upper and lower mantle convective flow. Interestingly, the predicted ice volume change based on the total dynamic topography signal is not the same as the sum of changes associated with the upper and lower mantle convection simulations. This suggests significant non-linear coupling between bedrock elevation and ice sheet stability in both the Greenland and Antarctic simulations.

Present-day dynamic topography is unlikely to be unique in its scale or spatial distribution, and in previous time periods it could be as important in modulating the state of ice sheets. Considering the spatial distribution of ice sheet retreat and advance in our models, areas which are dynamically uplifted tend to gain ice mass, while areas which are subsided tend to lose mass, a

trend which we expect would also hold for earlier time periods. When modeling ice sheets during previous icehouse periods in Earth’s history or early in the current one (e.g. DeConto et al., 2008), our results suggest that the choice of dynamic topography model may be as important as climate forcing in determining the equilibrium ice sheet state. In polar regions, dynamic topography can enhance or suppress a significant amount of ice; moreover, on a global scale, mean sea level changes due to dynamic topography altering ocean volume and seafloor position would affect the grounding lines of any marine-based ice sheets. The increased uncertainty of dynamic topography in progressively earlier icehouse periods introduces significant uncertainty in any deep-time ice sheet reconstructions. Supplemental tests (figures S17 and S18) show that re-adding dynamic topography after removing it causes the ice sheets evolve to positions similar to the pre-industrial present-day equilibrium state, implying that future studies can to some extent quantify the impact of uncertainty in dynamic topography reconstruction on ice sheet equilibria simply by adding in different dynamic topography models using the methodology of this study and comparing equilibrium states.

Our modeling in Antarctica reinforces previous work in this region highlighting the importance of dynamic topography in shaping the Antarctic ice sheet (Austermann et al., 2015; Fox et al., 2024). Fox et al. (2024) find that removing geologically-inferred changes in dynamic topography since the inception of glaciation in the Antarctic Peninsula causes a significant redistribution of ice. The large differences in predicted ice sheet configuration between their work and the present study arises from the different time scale of focus: dynamic topography change since glacial inception versus the instantaneous present-day signal.

Dynamic topography is less important to the equilibrium state of the Greenland Ice Sheet than it is to the Antarctic ice sheet, despite experiencing dynamic topography signals comparable to the magnitude of Antarctica. In Greenland simulations there is comparatively little change in grounded ice extent, with only a ~ 0.20 chance of moderate retreat in the northeast. Though ice sheet-elevation effects lead to moderate changes in ice thickness over the extent of the ice sheet in all our simulations, the feedback effects there are insufficient to significantly alter the ice sheet extent. Our results are in contrast to Steinberger et al. (2015), which has shown the importance of dynamic topography on pre-conditioning glacial inception. This difference suggests that near a tipping point of the Greenland volume hysteresis loop (Robinson et al., 2012) dynamic topography can cause a transition from one regime to another, but away from those points, the ice sheet remains relatively stable.

The limitations of the present study include a relatively coarse resolution in the ice sheet modeling due to computational cost and our assumption of uniform lithosphere structure in the

GIA modeling. In future work considering the impacts of dynamic topography on ice sheets during earlier time periods, one can make use of improved retrodictions of dynamic topography generated using adjoint methods, such as Ghelichkhan et al. (2021), alongside the tools developed in this study. In any case, our results demonstrate the importance of dynamic topography and Earth’s internal dynamics in modulating the equilibrium state of the Earth’s ice sheets and consequently the Earth system as a whole.

Acknowledgments

We would like to thank David Pollard for technical support in using the PSUICE3D model, and would also like to thank Bernhard Steinberger and an anonymous reviewer for their feedback on this manuscript.

B.P. is supported by a Tomlinson Doctoral Fellowship from McGill University; B.P. and N.G. are supported by Natural Sciences and Engineering Research Council of Canada grant RGPIN-2016-05159 and the Canada Research Chairs program grant 241814; M.J.H. is supported by an Australian Research Council *Discovery Early Career Researcher Award* (DE220101519). This research was performed on unceded Kanein’kehá:ka and Massachusee land.

Data availability

All data and code necessary to reproduce the figures and analysis of this paper are available as a zenodo repository, found at Parazin et al. (2025). Key data from all ice sheet model runs, including ice thickness, bed topography and basal sliding coefficients are available as NETCDF files. The whole mantle, upper mantle and lower mantle dynamic topography signals are additionally provided as csv files, in addition to csv files of all 15 whole-mantle dynamic topography models used in the sensitivity analysis.

Information needed to reproduce model runs is also provided. Input files necessary to run the ice sheet model, as well as the modified GIA model code and necessary input files for that model are additionally available in the same zenodo repository. The ice sheet model code itself can be found in the open data section of Gomez et al. (2024).

References

- Albrecht, T., Martin, M., Haseloff, M., Winkelmann, R., & Levermann, A. (2011). Parameterization for subgrid-scale motion of ice-shelf calving fronts [Journal Article]. *The Cryosphere*, 5(1), 35-44. Retrieved from <https://tc.copernicus.org/articles/5/35/2011/> (TC) doi: 10.5194/tc-5-35-2011
- Argus, D. F., Peltier, W. R., Drummond, R., & Moore, A. W. (2014). The Antarctica component of postglacial rebound model ICE-6G_C (VM5a) based on GPS positioning, exposure age dating of ice thicknesses, and relative sea level histories [Journal Article]. *Geophysical Journal International*, 198(1), 537-563. Retrieved from <https://doi.org/10.1093/gji/ggu140> doi: 10.1093/gji/ggu140
- Austermann, J., & Mitrovica, J. X. (2015). Calculating gravitationally self-consistent sea level changes driven by dynamic topography [Journal Article]. *Geophysical Journal International*, 203(3), 1909-1922. Retrieved from <https://doi.org/10.1093/gji/ggv371> doi: 10.1093/gji/ggv371
- Austermann, J., Pollard, D., Mitrovica, J. X., Moucha, R., Forte, A. M., DeConto, R. M., ... Raymo, M. E. (2015). The impact of dynamic topography change on Antarctic ice sheet stability during the mid-Pliocene warm period [Journal Article]. *Geology*, 43(10), 927-930. Retrieved from <https://doi.org/10.1130/G36988.1> doi: 10.1130/g36988.1
- Bamber, J. L., Griggs, J. A., Hurkmans, R. T. W. L., Dowdeswell, J. A., Gogineni, S. P., Howat, I., ... Steinhage, D. (2013). A new bed elevation dataset for Greenland [Journal Article]. *The Cryosphere*, 7(2), 499-510. Retrieved from <https://tc.copernicus.org/articles/7/499/2013/> (TC) doi: 10.5194/tc-7-499-2013
- Barletta, V. R., Bevis, M., Smith, B. E., Wilson, T., Brown, A., Bordoni, A., ... Wiens, D. A. (2018). Observed rapid bedrock uplift in Amundsen Sea Embayment promotes ice-sheet stability [Journal Article]. *Science*, 360(6395), 1335-1339. Retrieved from <https://www.science.org/doi/abs/10.1126/science.aao1447> doi: 10.1126/science.aao1447
- Braun, J. (2010). The many surface expressions of mantle dynamics. *Nature Geoscience*, 3(12), 825-833.
- Colleoni, F., De Santis, L., Montoli, E., Olivo, E., Sorlien, C. C., Bart, P. J., ... Prato, S. (2018). Past continental shelf evolution increased Antarctic ice sheet sensitivity to climatic conditions [Journal Article]. *Scientific Reports*, 8(1), 11323. Retrieved from <https://doi.org/10.1038/s41598-018-29718-7> doi: 10.1038/s41598-018-29718-7
- Cooper, M. A., Jordan, T. M., Schroeder, D. M., Siegert, M. J., Williams, C. N., & Bamber, J. L. (2019). Subglacial roughness of the Greenland Ice Sheet: relationship with con-

temporary ice velocity and geology. *The Cryosphere*, 13(11), 3093–3115. Retrieved from
<https://tc.copernicus.org/articles/13/3093/2019/> doi: 10.5194/tc-13-3093-2019

Corrieu, V., Thoraval, C., & Ricard, Y. (1995). Mantle dynamics and geoid Green functions.
Geophysical Journal International, 120(2), 516–523.

Coulon, V., Bulthuis, K., Whitehouse, P. L., Sun, S., Haubner, K., Zipf, L., & Pattyn, F.
 (2021). Contrasting response of West and East Antarctic ice sheets to glacial isostatic
 adjustment. *Journal of Geophysical Research: Earth Surface*, 126(7), e2020JF006003.

Coulson, S. (2021). Geodynamic Insights on Critical Climate Events in Earth History.
ProQuest Dissertations and Theses, 152. Retrieved from [https://proxy.library](https://proxy.library.mcgill.ca/login?url=https://www.proquest.com/dissertations-theses/geodynamic-insights-on-critical-climate-events/docview/2564445657/se-2)
[.mcgill.ca/login?url=https://www.proquest.com/dissertations-theses/](https://proxy.library.mcgill.ca/login?url=https://www.proquest.com/dissertations-theses/geodynamic-insights-on-critical-climate-events/docview/2564445657/se-2)
[geodynamic-insights-on-critical-climate-events/docview/2564445657/se-2](https://proxy.library.mcgill.ca/login?url=https://www.proquest.com/dissertations-theses/geodynamic-insights-on-critical-climate-events/docview/2564445657/se-2)
 (Copyright - Database copyright ProQuest LLC; ProQuest does not claim copyright in
 the individual underlying works; Last updated - 2023-06-22)

Davies, D. R., Valentine, A., Kramer, S. C., Rawlinson, N., Hoggard, M., Eakin, C., & Wil-
 son, C. (2019). Earth’s multi-scale topographic response to global mantle flow. *Nature*
Geoscience, 12(10), 845–850.

Durand, G., Gagliardini, O., de Fleurian, B., Zwinger, T., & Le Meur, E. (2009). Marine
 ice sheet dynamics: Hysteresis and neutral equilibrium. *Journal of Geophysical Research:*
Earth Surface, 114(F3). Retrieved from [https://agupubs.onlinelibrary.wiley.com/](https://agupubs.onlinelibrary.wiley.com/doi/abs/10.1029/2008JF001170)
[doi/abs/10.1029/2008JF001170](https://agupubs.onlinelibrary.wiley.com/doi/abs/10.1029/2008JF001170) doi: <https://doi.org/10.1029/2008JF001170>

Dziewonski, A. M., Chou, T.-A., & Woodhouse, J. H. (1981). Determination of earthquake
 source parameters from waveform data for studies of global and regional seismicity. *Jour-*
nal of Geophysical Research: Solid Earth, 86(B4), 2825–2852.

Elson, P., Sales De Andrade, E., Hattersley, R., Campbell, E., May, R., Dawson, A., ...
 others (2023). SciTools/cartopy: Cartopy 0.18.0 [Software]. *Zenodo*.

Fox, M., Clinger, A., Smith, A. G. G., Cuffey, K., Shuster, D., & Herman, F. (2024). Antarc-
 tic Peninsula glaciation patterns set by landscape evolution and dynamic topography
 [Journal Article]. *Nature Geoscience*, 17(1), 73-78. Retrieved from [https://doi.org/](https://doi.org/10.1038/s41561-023-01336-7)
[10.1038/s41561-023-01336-7](https://doi.org/10.1038/s41561-023-01336-7) doi: 10.1038/s41561-023-01336-7

Fretwell, P., Pritchard, H. D., Vaughan, D. G., Bamber, J. L., Barrand, N. E., Bell, R.,
 ... Zirizzotti, A. (2013). Bedmap2: improved ice bed, surface and thickness datasets
 for Antarctica [Journal Article]. *The Cryosphere*, 7(1), 375-393. Retrieved from
<https://tc.copernicus.org/articles/7/375/2013/> (TC) doi: 10.5194/tc-7-375-2013

Ghelichkhan, S., Bunge, H.-P., & Oeser, J. (2021). Global mantle flow retrodictions for
 the early Cenozoic using an adjoint method: evolving dynamic topographies, deep mantle

- structures, flow trajectories and sublithospheric stresses [Journal Article]. *Geophysical Journal International*, 226(2), 1432-1460. Retrieved from <https://doi.org/10.1093/gji/ggab108> doi: 10.1093/gji/ggab108
- Gomez, N., Mitrovica, J. X., Tamisiea, M. E., & Clark, P. U. (2010). A new projection of sea level change in response to collapse of marine sectors of the Antarctic Ice Sheet [Journal Article]. *Geophysical Journal International*, 180(2), 623-634. Retrieved from <https://doi.org/10.1111/j.1365-246X.2009.04419.x> doi: 10.1111/j.1365-246X.2009.04419.x
- Gomez, N., Pollard, D., & Holland, D. (2015). Sea-level feedback lowers projections of future Antarctic Ice-Sheet mass loss [Journal Article]. *Nature Communications*, 6(1), 8798. Retrieved from <https://doi.org/10.1038/ncomms9798> doi: 10.1038/ncomms9798
- Gomez, N., Pollard, D., & Mitrovica, J. X. (2013). A 3-D coupled ice sheet–sea level model applied to Antarctica through the last 40 ky. *Earth and Planetary Science Letters*, 384, 88–99.
- Gomez, N., Yousefi, M., Pollard, D., DeConto, R. M., Sadai, S., Lloyd, A., ... Wilson, T. (2024). The influence of realistic 3D mantle viscosity on Antarctica’s contribution to future global sea levels [Journal Article]. *Science Advances*, 10(31), eadn1470. Retrieved from <https://www.science.org/doi/abs/10.1126/sciadv.adn1470> doi: 10.1126/sciadv.adn1470
- Grand, S. P. (2002). Mantle shear-wave tomography and the fate of subducted slabs. *Philosophical Transactions of the Royal Society of London. Series A: Mathematical, Physical and Engineering Sciences*, 360(1800), 2475–2491.
- Gurnis, M. (1990). Bounds on global dynamic topography from Phanerozoic flooding of continental platforms. *Nature*, 344(6268), 754–756.
- Hager, B. H., Clayton, R. W., Richards, M. A., Comer, R. P., & Dziewonski, A. M. (1985). Lower mantle heterogeneity, dynamic topography and the geoid. *Nature*, 313(6003), 541–545.
- Hager, B. H., & O’Connell, R. J. (1981). A simple global model of plate dynamics and mantle convection. *Journal of Geophysical Research: Solid Earth*, 86(B6), 4843–4867.
- Han, H. K., Gomez, N., & Wan, J. X. W. (2022). Capturing the interactions between ice sheets, sea level and the solid Earth on a range of timescales: a new “time window” algorithm [Journal Article]. *Geosci. Model Dev.*, 15(3), 1355-1373. Retrieved from <https://gmd.copernicus.org/articles/15/1355/2022/> (GMD) doi: 10.5194/gmd-15-1355-2022
- Hoggard, M. J., Winterbourne, J., Czarnota, K., & White, N. (2017). Oceanic residual depth measurements, the plate cooling model, and global dynamic topography. *Journal of Geo-*

- 472 *physical Research: Solid Earth*, 122(3), 2328–2372.
- 473 Ignéczi, Á., Sole, A. J., Livingstone, S. J., Ng, F. S., & Yang, K. (2018). Greenland Ice Sheet
474 surface topography and drainage structure controlled by the transfer of basal variability.
475 *Frontiers in Earth Science*, 6, 101.
- 476 Kendall, R. A., Mitrovica, J. X., & Milne, G. A. (2005). On post-glacial sea level – II. Nu-
477 merical formulation and comparative results on spherically symmetric models [Journal
478 Article]. *Geophysical Journal International*, 161(3), 679–706. Retrieved from [https://](https://doi.org/10.1111/j.1365-246X.2005.02553.x)
479 doi.org/10.1111/j.1365-246X.2005.02553.x doi: 10.1111/j.1365-246X.2005.02553.x
- 480 Le Brocq, A. M., Payne, A. J., & Vieli, A. (2010). An improved Antarctic dataset for high
481 resolution numerical ice sheet models (ALBMAP v1) [Journal Article]. *Earth Syst. Sci.*
482 *Data*, 2(2), 247–260. Retrieved from [https://essd.copernicus.org/articles/2/247/](https://essd.copernicus.org/articles/2/247/2010/)
483 [2010/](https://essd.copernicus.org/articles/2/247/2010/) (ESSD) doi: 10.5194/essd-2-247-2010
- 484 Lecavalier, B. S., Milne, G. A., Simpson, M. J. R., Wake, L., Huybrechts, P., Tarasov, L., ...
485 Larsen, N. K. (2014). A model of Greenland ice sheet deglaciation constrained by obser-
486 vations of relative sea level and ice extent [Journal Article]. *Quaternary Science Reviews*,
487 102, 54–84. Retrieved from [https://www.sciencedirect.com/science/article/pii/](https://www.sciencedirect.com/science/article/pii/S0277379114003011)
488 [S0277379114003011](https://www.sciencedirect.com/science/article/pii/S0277379114003011) doi: <https://doi.org/10.1016/j.quascirev.2014.07.018>
- 489 Levitus, S., Antonov, J. I., Boyer, T. P., Baranova, O. K., Garcia, H. E., Locarnini, R. A.,
490 ... Zweng, M. M. (2012). World ocean heat content and thermosteric sea level change
491 (0–2000 m), 1955–2010 [Journal Article]. *Geophysical Research Letters*, 39(10). Retrieved
492 from <https://agupubs.onlinelibrary.wiley.com/doi/abs/10.1029/2012GL051106>
493 doi: <https://doi.org/10.1029/2012GL051106>
- 494 Lloyd, A. J., Wiens, D. A., Zhu, H., Tromp, J., Nyblade, A. A., Aster, R. C., ... others
495 (2020). Seismic structure of the Antarctic upper mantle imaged with adjoint tomography.
496 *Journal of Geophysical Research: Solid Earth*, 125(3).
- 497 Mercer, J. H. (1978). West Antarctic ice sheet and CO₂ greenhouse effect: a threat of disas-
498 ter. *Nature*, 271(5643), 321–325.
- 499 Mitrovica, J. X., Austermann, J., Coulson, S., Creveling, J., Hoggard, M., Jarvis, G., &
500 Richards, F. (2020). Dynamic Topography and Ice Age Paleoclimate [Journal Arti-
501 cle]. *Annual Review of Earth and Planetary Sciences*, 48(1), 585–621. Retrieved from
502 <https://www.annualreviews.org/doi/abs/10.1146/annurev-earth-082517-010225>
503 doi: 10.1146/annurev-earth-082517-010225
- 504 Mitrovica, J. X., Beaumont, C., & Jarvis, G. (1989). Tilting of continental interiors by the
505 dynamical effects of subduction. *Tectonics*, 8(5), 1079–1094.
- 506 Mitrovica, J. X., & Milne, G. A. (2003). On post-glacial sea level: I. General theory [Journal

- Article]. *Geophysical Journal International*, 154(2), 253-267. Retrieved from <https://doi.org/10.1046/j.1365-246X.2003.01942.x> doi: 10.1046/j.1365-246X.2003.01942.x
- Morland, L., & Johnson, I. (1982). Effects of bed inclination and topography on steady isothermal ice sheets. *Journal of Glaciology*, 28(98), 71–90.
- Morlighem, M., et al. (2020). Measures bedmachine antarctica, version 2. *Boulder, Color. USA. NASA Natl. Snow Ice Data Cent. Distrib. Act. Arch. Cent*, 10, E1QL9HFQ7A8M.
- Morlighem, M., Rignot, E., Binder, T., Blankenship, D., Drews, R., Eagles, G., ... others (2020). Deep glacial troughs and stabilizing ridges unveiled beneath the margins of the Antarctic ice sheet. *Nature geoscience*, 13(2), 132–137.
- Morlighem, M., Williams, C. N., Rignot, E., An, L., Arndt, J. E., Bamber, J. L., ... others (2017). BedMachine v3: Complete bed topography and ocean bathymetry mapping of Greenland from multibeam echo sounding combined with mass conservation. *Geophysical research letters*, 44(21), 11–051.
- NGDC. (2006). 2-minute gridded global relief data (ETOPO2) v2. *National Geophysical Data Center, NOAA..*
- Nick, F., Van Der Veen, C., Vieli, A., & Benn, D. (2010). A physically based calving model applied to marine outlet glaciers and implications for the glacier dynamics. *Journal of Glaciology*, 56(199), 781–794. doi: 10.3189/002214310794457344
- Noël, B., Van De Berg, W. J., Van Wessem, J. M., Van Meijgaard, E., Van As, D., Lenaerts, J., ... others (2018). Modelling the climate and surface mass balance of polar ice sheets using RACMO2–Part 1: Greenland (1958–2016). *The Cryosphere*, 12(3), 811–831.
- Parazin, B., Gomez, N., Richards, F., Coulson, S., Hoggard, M., & Mitrovica, J. (2025, April). *Data for Ice Sheets without Dynamic topography [Dataset and Software]*. Zenodo. Retrieved from <https://doi.org/10.5281/zenodo.15212720> doi: 10.5281/zenodo.15212720
- Paxman, G. J. G., Gasson, E. G. W., Jamieson, S. S. R., Bentley, M. J., & Ferraccioli, F. (2020). Long-Term Increase in Antarctic Ice Sheet Vulnerability Driven by Bed Topography Evolution. *Geophysical Research Letters*, 47(20), e2020GL090003. Retrieved from <https://agupubs.onlinelibrary.wiley.com/doi/abs/10.1029/2020GL090003> (e2020GL090003 2020GL090003) doi: <https://doi.org/10.1029/2020GL090003>
- Paxman, G. J. G., Jamieson, S. S. R., Hochmuth, K., Gohl, K., Bentley, M. J., Leitchenkov, G., & Ferraccioli, F. (2019). Reconstructions of Antarctic topography since the Eocene-Oligocene boundary. *Palaeogeography, Palaeoclimatology, Palaeoecology*, 535, 109346. Retrieved from <https://www.sciencedirect.com/science/article/pii/S0031018219304845> doi: <https://doi.org/10.1016/j.palaeo.2019.109346>

542 Peltier, W. R., Argus, D. F., & Drummond, R. (2015). Space geodesy constrains
543 ice age terminal deglaciation: The global ICE-6G_C (VM5a) model [Journal Arti-
544 cle]. *Journal of Geophysical Research: Solid Earth*, 120(1), 450-487. Retrieved from
545 <https://agupubs.onlinelibrary.wiley.com/doi/abs/10.1002/2014JB011176> doi:
546 <https://doi.org/10.1002/2014JB011176>

547 Pollard, D., Chang, W., Haran, M., Applegate, P., & DeConto, R. (2016). Large ensem-
548 ble modeling of the last deglacial retreat of the West Antarctic Ice Sheet: comparison of
549 simple and advanced statistical techniques [Journal Article]. *Geosci. Model Dev.*, 9(5),
550 1697-1723. Retrieved from <https://gmd.copernicus.org/articles/9/1697/2016/>
551 (GMD) doi: 10.5194/gmd-9-1697-2016

552 Pollard, D., & DeConto, R. M. (2012a). Description of a hybrid ice sheet-shelf model, and
553 application to Antarctica [Journal Article]. *Geosci. Model Dev.*, 5(5), 1273-1295. Retrieved
554 from <https://gmd.copernicus.org/articles/5/1273/2012/> (GMD) doi: 10.5194/gmd
555 -5-1273-2012

556 Pollard, D., & DeConto, R. M. (2012b). A simple inverse method for the distribution of
557 basal sliding coefficients under ice sheets, applied to Antarctica [Journal Article]. *The*
558 *Cryosphere*, 6(5), 953-971. Retrieved from [https://tc.copernicus.org/articles/6/](https://tc.copernicus.org/articles/6/953/2012/)
559 [953/2012/](https://tc.copernicus.org/articles/6/953/2012/) (TC) doi: 10.5194/tc-6-953-2012

560 Pollard, D., & DeConto, R. M. (2020). Improvements in one-dimensional grounding-line
561 parameterizations in an ice-sheet model with lateral variations (PSUICE3D v2.1). *Geosci-*
562 *entific Model Development*, 13(12), 6481-6500. Retrieved from [https://gmd.copernicus](https://gmd.copernicus.org/articles/13/6481/2020/)
563 [.org/articles/13/6481/2020/](https://gmd.copernicus.org/articles/13/6481/2020/) doi: 10.5194/gmd-13-6481-2020

564 Pollard, D., Gomez, N., & Deconto, R. M. (2017). Variations of the Antarctic Ice Sheet
565 in a Coupled Ice Sheet-Earth-Sea Level Model: Sensitivity to Viscoelastic Earth Proper-
566 ties [Journal Article]. *Journal of Geophysical Research: Earth Surface*, 122(11), 2124-
567 2138. Retrieved from [https://agupubs.onlinelibrary.wiley.com/doi/abs/10.1002/](https://agupubs.onlinelibrary.wiley.com/doi/abs/10.1002/2017JF004371)
568 [2017JF004371](https://agupubs.onlinelibrary.wiley.com/doi/abs/10.1002/2017JF004371) doi: <https://doi.org/10.1002/2017JF004371>

569 Richards, F. D., Hoggard, M. J., Ghelichkhan, S., Koelemeijer, P., & Lau, H. C. P. (2023).
570 Geodynamic, geodetic, and seismic constraints favour deflated and dense-cored LLVPs
571 [Journal Article]. *Earth and Planetary Science Letters*, 602, 117964. Retrieved from
572 <https://www.sciencedirect.com/science/article/pii/S0012821X22006008> doi:
573 <https://doi.org/10.1016/j.epsl.2022.117964>

574 Richards, F. D., Hoggard, M. J., White, N., & Ghelichkhan, S. (2020). Quantifying the
575 Relationship Between Short-Wavelength Dynamic Topography and Thermomechanical
576 Structure of the Upper Mantle Using Calibrated Parameterization of Anelasticity [Journal

- Article]. *Journal of Geophysical Research: Solid Earth*, 125(9), e2019JB019062. Retrieved from <https://agupubs.onlinelibrary.wiley.com/doi/abs/10.1029/2019JB019062> doi: <https://doi.org/10.1029/2019JB019062>
- Robel, A. A., Seroussi, H., & Roe, G. H. (2019). Marine ice sheet instability amplifies and skews uncertainty in projections of future sea-level rise. *Proceedings of the National Academy of Sciences*, 116(30), 14887-14892. Retrieved from <https://www.pnas.org/doi/abs/10.1073/pnas.1904822116> doi: 10.1073/pnas.1904822116
- Robinson, A., Calov, R., & Ganopolski, A. (2012). Multistability and critical thresholds of the Greenland ice sheet. *Nature Climate Change*, 2(6), 429-432.
- Schoof, C. (2007). Ice sheet grounding line dynamics: Steady states, stability, and hysteresis [Journal Article]. *Journal of Geophysical Research: Earth Surface*, 112(F3). Retrieved from <https://agupubs.onlinelibrary.wiley.com/doi/abs/10.1029/2006JF000664> doi: <https://doi.org/10.1029/2006JF000664>
- Steinberger, B. (2016, 01). Topography caused by mantle density variations: observation-based estimates and models derived from tomography and lithosphere thickness. *Geophysical Journal International*, 205(1), 604-621. Retrieved from <https://doi.org/10.1093/gji/ggw040> doi: 10.1093/gji/ggw040
- Steinberger, B., Spakman, W., Japsen, P., & Torsvik, T. H. (2015). The key role of global solid-Earth processes in preconditioning Greenland's glaciation since the Pliocene. *Terra Nova*, 27(1), 1-8.
- Steinberger, B., Werner, S. C., & Torsvik, T. H. (2010). Deep versus shallow origin of gravity anomalies, topography and volcanism on Earth, Venus and Mars. *Icarus*, 207(2), 564-577.
- van Meijgaard, E., Van Uft, L., Van de Berg, W., Bosveld, F., Van den Hurk, B., Lenderink, G., & Siebesma, A. (2008). *The KNMI regional atmospheric climate model RACMO, version 2.1*. KNMI De Bilt, The Netherlands.
- Weertman, J. (1961). Stability of ice-age ice sheets. *Journal of Geophysical Research*, 66(11), 3783-3792.
- Weertman, J. (1974). Stability of the junction of an ice sheet and an ice shelf. *Journal of Glaciology*, 13(67), 3-11.
- Zeitz, M., Haacker, J. M., Donges, J. F., Albrecht, T., & Winkelmann, R. (2022). Dynamic regimes of the Greenland Ice Sheet emerging from interacting melt-elevation and glacial isostatic adjustment feedbacks. *Earth System Dynamics*, 13(3), 1077-1096. Retrieved from <https://esd.copernicus.org/articles/13/1077/2022/> doi: 10.5194/esd-13-1077-2022